IF Estimation for Multicomponent Signals Using Image Processing Techniques in the Time–Frequency Domain ⋆

L. Rankine [a,*] , M. Mesbah [a], B. Boashash [a,b]

[a] *Perinatal Research Centre, University of Queensland, Royal Brisbane and Women's Hospital, Brisbane, QLD 4029, Australia.*

[b] *College of Engineering, University of Sharjah, Sharjah, UAE.*

Abstract

This paper presents a method for estimating the instantaneous frequency (IF) of multicomponent signals. The technique involves, firstly, the transformation of the one dimensional signal to the two dimensional time–frequency domain using a reduced interference quadratic time–frequency distribution. IF estimation of signal components is then achieved by implementing two image processing steps: local peak detection of the time–frequency (TF) representation followed by an image processing technique called component linking. The proposed IF estimator is tested on noisy synthetic monocomponent and multicomponent signals exhibiting linear and nonlinear laws. For low signal to noise ratio (SNR) environments, a time–frequency peak filtering preprocessing step is used for signal enhancement. Application of the IF estimation scheme to real signals is illustrated with newborn EEG signals. Finally, to illustrate the potential use of the proposed IF estimation method in classifying signals based on their TF components' IFs, a classification method using least squares data–fitting is proposed and illustrated on synthetic and real signals.

Key words: instantaneous frequency, multicomponent signals, time–frequency representation, image processing, EEG

⋆ This work was supported through grants from the NHMRC and ARC.

* Corresponding author. Tel. +61 7 3346 4948, Fax. +61 3636 2123
Email address: lrankine@somc.uq.edu.au (L. Rankine).
URL: http://www.som.uq.edu.au/research/sprcg (L. Rankine).

1 Introduction

The IF is a signal parameter which is of significant importance in many real applications, such as radar, sonar, telecommunications and biomedicine [1]. For an analytic [2], monocomponent signal,

$$z(t) = a(t)e^{j\phi(t)} \tag{1}$$

the instantaneous frequency is defined as

$$f_i(t) = \frac{1}{2\pi}\frac{d\phi(t)}{dt} \tag{2}$$

where $a(t)$ and $\phi(t)$ are two real functions that are referred to as the instantaneous amplitude and instantaneous phase respectively.

A review of techniques for estimating the IF, such as phase difference estimators, zero crossing–based IF estimation, adaptive parameterization methods and TF based techniques, can be found in [3]. Among those, TF based IF estimation techniques have received considerable attention recently, as illustrated by the papers [4–10].

As discussed in [1], an ideal TF representation of a monocomponent signal of the form (1) would exhibit a peak about the IF, with an amplitude related to the signal envelope. It has been shown that some quadratic time–frequency distributions (QTFDs), such as the Wigner–Ville distribution (WVD) and modified B-distribution (MBD) [11, 12], provide a peak centered at the IF for linear frequency modulated (LFM) signals. Therefore, an intuitive method for estimating the IF is to take the peak of these QTFDs, as described in [3]. However, care must be taken with nonlinear frequency modulated signal components as the peak estimate is biased (see [5, 6, 12] for further details).

Consider now a multicomponent signal, $z(t)$, composed of a sum of monocomponent signals corrupted with complex–valued additive white Gaussian noise, $r(t)$, with independently and identically distributed (i.i.d) real and imaginary parts, such that

$$z(t) = \sum_{i=1}^{M} a_i(t)e^{j\phi_i(t)} + r(t) \tag{3}$$

where $a_i(t)$ and $\phi_i(t)$ are the amplitude envelope and instantaneous phase of the i^{th} signal component respectively and M is the number of signal components. In this paper, we classify a multicomponent signal as being either TF separable or TF nonseparable. A TF nonseparable signal is defined as a signal whose TF components are either too close to separate in the TF domain or with components that actually intersect. A TF separable multicomponent signal is, however, a signal whose TF components are clearly separated in the TF

domain and hence possess a unique TF decomposition. We restrict our present study to the case of TF separable multicomponent (referred to from this point on as just multicomponent) signals whose TF components are characterized by continuous IFs. This characteristic is shared by most physiological signals such as newborn EEG [13] and heart rate variability [14].

The idea of a single IF for a multicomponent signal, as defined by (3), becomes a meaningless [1]. Instead, estimation of the IF of each individual component is the desired information to be extracted from multicomponent signals.

Component IF estimation for multicomponent signals using the local peaks of QTFDs has previously been proposed. In [12], an adaptive QTFD was presented and local peaks were used to estimate the IF of components. However, this method requires *a priori* information about the ratio between signal component amplitudes, assuming the component amplitudes are constant, so that local maxima caused by crossterms and noise can be ignored by setting an appropriate threshold level [12]. For this reason, the method was not assessed with low signal to noise ratio (SNR) signals or real signals with time–varying amplitudes.

The two dimensional representation of a signal in the joint TF domain has led to the use of pattern recognition techniques to extract the individual IFs of multicomponent signals. In [7], the authors developed a method for estimating the parameters associated with LFM signals using a Wigner–Hough transform. This technique was extended in [8] to be applicable to nonlinear frequency modulated signals. In [9], the authors proposed a combined Hough–Radon transform of a positive time–frequency distribution to estimate multicomponent IFs. The authors in [10] developed a technique for multicomponent IF estimation based on the randomized Hough transform (RHT) of the TF representation, using edge information obtained from matched filtering-based edge detection to eliminate spurious votes in the RHT.

The Hough transform, used in each of the methods presented in [7–10], is a well known method for finding curves in images [15]. However, the Hough transform requires *a priori* information about the class of IF law (*e.g. linear, quadratic, cubic, hyperbolic, sinusoidal etc.*) contained in the signal so that the TF representation can be transformed to the appropriate Hough parameter space. This means that the component IF laws of a signal which contains, for example, a component with a linear IF law and a component with a sinusoidal IF law, cannot both be accurately estimated simultaneously. The IF estimation methods incorporating the Hough transform also provide poor results if the IF of a signal component is not easily represented by a parametric function [9].

This paper proposes a new technique for multicomponent IF estimation without requiring a threshold to be set for local peaks in the TF domain or *a priori*

knowledge of the class of IF law. The technique involves a TF transformation of the signal using a high resolution, reduced interference QTFD. Component IFs are then extracted by a two step process: detection of local peaks in the TF representation to produce a binary image, followed by component linking. To allow for low SNR environments, a time–frequency peak filtering (TFPF) [16] preprocessing step is applied for signal enhancement.

The paper is organized as follows. Section 2 introduces QTFDs and TFPF preprocessing and gives a detailed description of the local peak detection and component linking algorithms that make up the proposed IF estimation technique. In section 3, the IF estimation algorithm is demonstrated on noisy synthetic monocomponent and multicomponent signals with components exhibiting linear and nonlinear IF laws. The performance of the proposed IF estimation when applied to real newborn EEG data is also given. In section 4, a method of classifying the extracted components IF laws using linear and nonlinear least squares data–fitting is outlined. A discussion and interpretation of the results obtained using the proposed IF estimation and component classification techniques are presented in section 5.

2 IF Estimation Algorithm

2.1 Quadratic Time–Frequency Distributions

QTFDs are commonly used for joint TF representation. The most basic QTFD is the Wigner–Ville distribution (WVD). All other QTFDs can be obtained by a TF averaging or smoothing of the WVD [17]. The general formula for a QTFD of a real signal, $s(t)$, is expressed as [17]

$$\rho_z(t,f) = \int_{-\infty}^{\infty}\int_{-\infty}^{\infty} G(t-u,\tau)z(u+\tfrac{\tau}{2})z^*(u-\tfrac{\tau}{2})e^{-j2\pi f\tau}dud\tau \qquad (4)$$

where $G(t,\tau)$ is the time–lag kernel which defines the QTFD and $z(t)$ is the analytic associate of $s(t)$ [18]. The WVD has the simplest time–lag kernel, expressed as $G(t,\tau)=\delta(t)$.

The WVD satisfies many mathematically desirable properties of a TF representation (see [17] for a detailed list of WVD properties). However, it also exhibits spurious features called crossterms which result from the bilinear nature of the Wigner-Ville TF transformation. In many applications, these crossterms can severely mask true signal components in the TF domain, resulting in a poor representation.

In [12], the authors proposed the time–lag kernel

$$G(t,\tau) = G_\beta(t) = \frac{\cosh^{-2\beta}(t)}{\int_{-\infty}^{\infty} \cosh^{-2\beta} \xi d\xi} \tag{5}$$

for a QTFD which retains high resolution of signal components while significantly reducing the effect of crossterms. The parameter, β, which satisfies $0 < \beta \leq 1$, controls the resolution–crossterm elimination tradeoff in the distribution. It was also shown in [12] that this distribution, referred from here on as the modified B-distribution (MBD), produces a peak along the IF for LFM components. For the proposed IF estimation algorithm, the MBD will be used to represent signals in the TF domain.

2.2 Time–Frequency Peak Filtering

TFPF was proposed in [16, 19] as a preprocessing method for enhancing a signal buried in noise at low SNR. The algorithm consists of two basic steps:

(1) Encode the real noisy signal, $s(t)$, via frequency modulation as:

$$z_s(t) = e^{j2\pi\mu \int_{-\infty}^{t} s(\lambda) d\lambda} \tag{6}$$

where μ is a scaling parameter analogous to the frequency modulation index.

(2) Estimate the peak of the WVD of the analytic, monocomponent signal $z_s(t)$:

$$\hat{s}(t) = \hat{f_{z_s}}(t) = \frac{\arg\max_f [W_{z_s}(t,f)]}{\mu} \tag{7}$$

where $W_{z_s}(t,f)$ is the WVD of $z_s(t)$. The reason for choosing the WVD in the TFPF procedure is that the encoded signal, $z_s(t)$, is monocomponent with fast variations in the IF. It was recently shown that the WVD outperformed other reduced interference QTFDs in estimating the IF of monocomponent signals for the case where the IF changed rapidly [6]. The use of the WVD in the TFPF should not be confused with the use of the MBD to represent the enhanced multicomponent signal, $\hat{s}(t)$, in the local peak estimation procedure described in the following subsection.

Discrete implementation of the TFPF method requires signal scaling to a range inside the band of normalized frequencies (*i.e.* [0,0.5]) before encoding to prevent aliasing [16]. The range [0.1,0.4] was chosen arbitrarily for the application of TFPF in this paper. In the discrete implementation of the TFPF procedure, the pseudo–WVD [11], rather than the WVD, is used so that a lag window length can be selected to reduce the bias in the estimate of the fast

changing IF of the encoded signal. To reduce the bias in the IF estimate in the TFPF procedure, the lag window length can be minimized or the sampling frequency increased [16]. However, reducing the lag window length increases the variance of the IF estimate [6]. In [16], a relationship between the maximum allowable window length for TFPF and the amount of oversampling for a desired maximum bias was derived. The valid lag window lengths for a maximum deviation of 20% across the kernel window was shown to be [16]

$$\tau_w \leq \frac{1.28 f_s}{\pi f_p} \tag{8}$$

where f_s is the sampling frequency and f_p is the maximum IF. From (8), it can be seen that the lag window length can be increased and, correspondingly, the variance can be reduced, for a given bias by increasing the sampling rate f_s. To minimize the variance, for all TFPF in this paper, we have oversampled the signal by 30 times before down sampling. The maximum lag window length for a signal 30 times over sampled, using (8), is given by $\tau_w \leq 24$ samples. Throughout this paper, we use a lag window length of 21 samples for the TFPF.

To improve the signal estimate in extremely low SNR, an iterative TFPF algorithm may be applied. This method simply repeats the TFPF process on the estimated signal until a satisfactory signal estimate is achieved. Convergence of the iterative TFPF algorithm has only been studied through simulations [16, 19]. It was found that suitable estimates of the signal occurred in approximately three or four iterations.

2.3 Local QTFD Peak Estimation and Component Linking

The TF representation, $\rho_{\hat{z}}(t,f)$, of the analytic associate, $\hat{z}(t)$, of time–frequency peak filtered signal, $\hat{s}(t)$, is obtained using the MBD. The MBD is then transformed into a binary image, $B(t,f)$, by assigning the locations of local peaks the value one, and assigning zero for all other locations. For the continuous TF representation, $\rho_{\hat{z}}(t,f)$, the binary image is given by the following conditions

$$B(t,f) = \begin{cases} 1 \ : \ if \ \left\{ \frac{\partial \rho_{\hat{z}}(t,f)}{\partial f} = 0 \right\} \bigoplus \left\{ \frac{\partial^2 \rho_{\hat{z}}(t,f)}{\partial f^2} < 0 \right\} \\ 0 \ : \ else \end{cases} \tag{9}$$

where $\bigoplus$ is the boolean AND operator.

The process of defining edges in images generally includes two steps: edge enhancement (*i.e.* binary transformation) followed by a component linking procedure [20]. The process of obtaining the binary image, $B(t,f)$, estimated

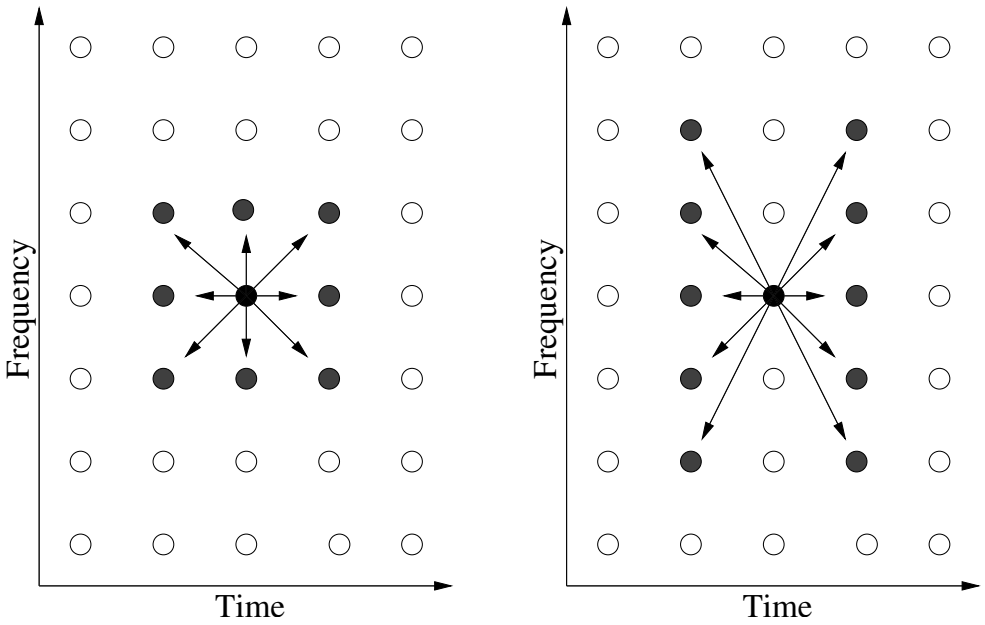

(a) 8-connected neighbouring set (b) 10-connected neighbouring set

Fig. 1. Illustration of connected neighbouring sets.

from the local peaks of $\rho_{\hat{z}}(t, f)$ can be thought of as an edge detection process.

A linked or connected component in a binary image is said to be a separate and independent object [21]. Using an 8-connected neighbouring set, any pixel (x, y) in a connected component has at least one other pixel with the coordinate in the set [21]

$$\begin{aligned} &\{(x-1, y-1), (x-1, y), (x-1, y+1), (x, y-1), \\ &(x, y+1), (x+1, y-1), (x+1, y), (x+1, y+1)\} \end{aligned} \tag{10}$$

The standard 8-connected neighbouring set is illustrated in Fig. 1(a)

A threshold for the number of connected pixels, P_L, which defines a true connected, or linked, component is generally set to remove falsely detected components. The threshold value is application dependent. For example, in component IF estimation, the number of pixels in a linked component is directly related to the time support of the signal component. Therefore, the threshold value is chosen as the minimum time duration for which a signal component can exist.

2.4 Discrete Analysis of Component Linking

2.4.1 Discrete modified B distribution

For implementation, the MBD must be discretized to provide a discrete QTFD of the form [22]

$$\rho_z[n,k] = 2 \underset{m \to k}{\mathrm{DFT}} \left\{ G[n,m] \underset{n}{\star} R_z[n,m] \right\} \tag{11}$$

where $\mathrm{DFT}\{\cdot\}$ is the discrete Fourier transform, $\underset{n}{\star}$ refers to convolution in n and $R_z[n,m]$ is the discrete instantaneous autocorrelation function (IAF), given as

$$R_z[n,m] = (z[n+m]z^*[n-m]) \tag{12}$$

The discrete time–lag kernel for the discrete MBD is given as

$$G[n,m] = G_\beta[n] = \frac{\cosh^{-2\beta} n}{\sum_n \cosh^{-2\beta} n} \tag{13}$$

For smoothing and localization [12], as well as improving the bias–variance tradeoff [5, 6], a window function, $w_h[m]$, of length h samples can be applied to the IAF, such that the discrete MBD is expressed as [22]

$$\rho_z,[n,k;w_h] = 2 \underset{m \to k}{\mathrm{DFT}} \left\{ G_\beta[n] \underset{n}{\star} (w_h[m] R_z[n,m]) \right\} \tag{14}$$

The number of frequency samples, which we refer to as the frequency resolution, in the discrete QTFD now becomes a function of window length, h. Larger window lengths allow for more data points in the DFT, therefore more frequency samples or higher frequency resolution. Shorter window lengths mean there are fewer data points for the DFT resulting in fewer frequency samples or lower frequency resolution.

2.4.2 Linking using an 8-connected neighbouring set

The linking of a component in a discrete QTFD is now shown to be dependent on the maximum of the first derivative of the IF. Consider a signal with N samples which is transformed to a discrete TF representation using the discrete MBD. The resulting discrete QTFD, $\rho_z[n,k;w_h]$, is an $N \times K$ matrix with N time samples and K frequency samples, where K is determined by the lag window length h in (14) (i.e. $K = h$, see [22] for details).

The interval, or period, between neighbouring samples along the time axis in

$\rho_z[n, k; w_h]$ is simply the sampling period given by

$$\Delta t = T_s = \frac{1}{f_s} \tag{15}$$

where f_s is the sampling frequency. The interval between neighbouring frequency samples is

$$\Delta f = \frac{f_s/2}{K} \tag{16}$$

Using an 8-connected neighbouring set, the maximum rate of change of the IF in either the positive or negative direction, such that the component can be linked, is one frequency sample, Δf, per time sample, Δt. That is,

$$\max\left\{\left|\frac{df_i(t)}{dt}\right|\right\} = \left|\frac{\pm\Delta f}{\Delta t}\right| \tag{17}$$

Substituting (15) and (16) into (17), we get

$$\max\left\{\left|\frac{df_i(t)}{dt}\right|\right\} = \frac{f_s^2}{2K} \tag{18}$$

The equation (18) suggests that $\max\left\{\left|\frac{df_i(t)}{dt}\right|\right\}$, such that a component can be linked using an 8-connected neighbouring set, is dependent on the sampling frequency, f_s, and the number of frequency samples in the discrete QTFD.

To increase $\max\left\{\left|\frac{df_i(t)}{dt}\right|\right\}$, the sampling frequency f_s can be increased or the number of frequency samples K can be decreased. Increasing the sampling frequency, f_s, results in the addition of irrelevant information, according to the Nyquist sampling theorem [23], and an increase in computation complexity. These are both undesirable.

Assuming that the bias for the IF estimate obtained from the peak of the discrete MBD is negligible, a decrease in the number of frequency samples, K, or frequency resolution, will result in an increase in Δf, as seen from (16). The mean square error (MSE) of the IF estimate caused by resolution error for uniform sampling of the frequency axis is [23]

$$\text{MSE} = \frac{\Delta f^2}{12} \tag{19}$$

which is the same error function associated with quantization errors. Therefore, decreasing K will significantly increase the mean square error of the IF estimate caused by the sampling of the frequency axis, which is highly undesirable.

2.4.3 Linking using a 10-connected neighbouring set

Consider now a new 10-connected neighbouring set

$$\begin{aligned}&\{(x-1,y-1),(x-1,y),(x-1,y+1),\\&(x+1,y-1),(x+1,y),(x+1,y+1)\\&(x-1,y-2),(x-1,y+2),(x+1,y-2),(x+1,y+2)\}\end{aligned} \tag{20}$$

where x and y represent the time and frequency axis respectively. This neighbouring set is illustrated in Fig. 1(b). This neighbouring set does not continue a search in the frequency direction only, as, by definition, there is only one instantaneous frequency at any given time instant for a signal component [1]. However, the maximum change in IF in either the positive or negative direction, which allows for component linking using the defined 10-connected neighbouring set, now becomes

$$\max\left\{\left|\frac{df_i(t)}{dt}\right|\right\} = \left|\frac{\pm 2\Delta f}{\Delta t}\right| = \frac{f_s^2}{K} \tag{21}$$

This results in a doubling of the allowable $\max\left\{\left|\frac{df_i(t)}{dt}\right|\right\}$, such that a component can still be linked, than is attainable with the 8-connected neighbouring set. In fact, by increasing the neighbouring set in this fashion, the $\max\left\{\left|\frac{df_i(t)}{dt}\right|\right\}$, such that a component can still be linked, can be continually increased. However, the issue of false component linking because of an excessively large neighbouring set, arises. The relationship between false component linking, $\max\left\{\left|\frac{df_i(t)}{dt}\right|\right\}$, and size of neighbouring set is beyond the scope of this paper but will be addressed in the future. Instead, we restrict the component linking algorithm to the use of the defined 10-connected neighbouring set in our proposed IF estimation algorithm. Simulations have demonstrated that false component linking using the 10-connected neighbouring set occurs only at very low SNR. However, low SNR is overcome by the TFPF preprocessing.

An example of a single connected component using the 10-connected neighbouring set is shown in Fig. 2. It can be seen from Fig. 2 that although the IF has changed rapidly from time $x = 4$ to $x = 5$, the component linking algorithm is able to link the component.

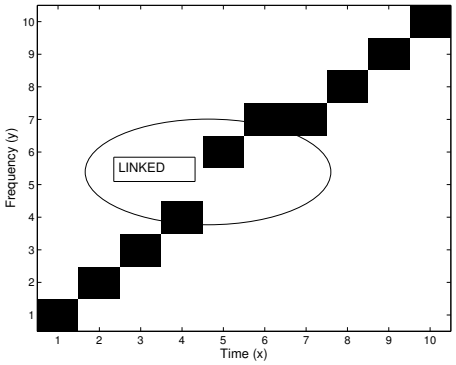

Fig. 2. A binary image showing a linked component using the 10-connected neighbouring set.

3 Performance Assessment and Discussion

3.1 Monocomponent Signal with 2^{nd} Order Polynomial Phase in WGN

The combined Wigner-Hough transform for IF estimation of 2^{nd} order polynomial phase, or LFM, signals was originally presented in [7]. The phase function for a LFM signal is given as

$$\phi_{\text{LFM}}(t) = 2\pi(f_0 + \tfrac{f_r}{2}t)t \tag{22}$$

where f_0 is the start frequency of the LFM and f_r is the linear frequency rate.

The performance assessment of the proposed IF estimation algorithm begins with a noisy, monocomponent LFM signal as it allows for 1) a comparison with the Cramer-Rao bound (CRB), calculated from [24] and 2) a direct comparison with the Wigner-Hough transform IF estimator [7]. IF estimation using the peak of the QTFD [1], in our case the MBD, was included in the comparison.

The LFM signal of length $N = 256$ samples used in this performance assessment has a sampling rate of $f_s = 1$Hz, a start frequency of $f_0 = 0.2$Hz, a frequency rate of $f_r = 3.9 \times 10^{-4}$Hz/s and unit amplitude. White Gaussian noise (WGN) was then added to the LFM signal to obtain noisy signals with signal to noise ratios (SNRs) in the range of 15dB down to -25dB.

Monte Carlo simulation was employed using 20 realizations of the noisy signal for each SNR. The results of the three IF estimators; namely, the peak of the MBD (Peak), the proposed component linking method (Linked) and the combined Wigner-Hough transform based method (WHT), with and without TFPF preprocessing, are presented in Fig. 3(a) and (b) respectively.

In this paper, unless otherwise stated, we have set the minimum length, in

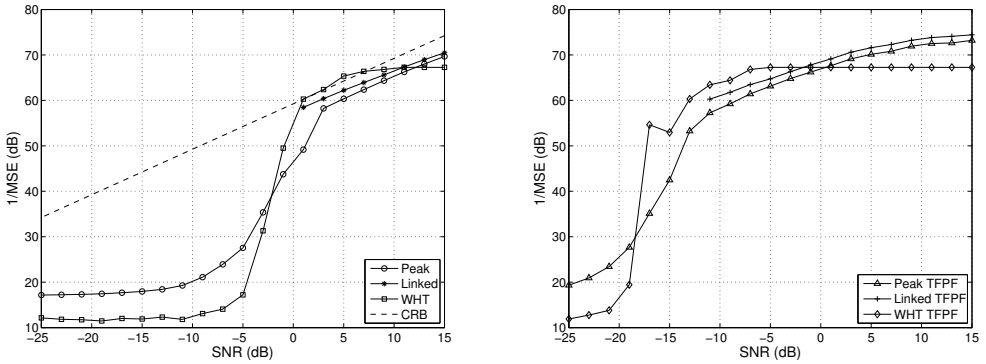

(a) No preprocessing (b) TFPF preprocessing

Fig. 3. MSE results from Monte Carlo simulations for three IF estimators; Peak of the MBD, component linking and Wigner-Hough transform with (a) no preprocessing and (b) TFPF preprocessing.

connected pixels, for a component to be considered a true signal component to be $P_L = \lfloor 3N/4 \rfloor$ samples. It can be seen in Fig. 3(a) that the Linked algorithm only provides IF estimates for SNR $\geq$ 1dB . For SNR $<$ 1dB the Linked algorithm fails to link a true component from the QTFD, therefore, no IF estimate can be achieved (see Fig. 3(a)). However, for SNR $\geq$ 1dB the Linked algorithm approximately follows the CRB. The MSE offset from the CRB for the Linked algorithm is a result of the resolution error caused by the discretization of the QTFD, as discussed in section 2.4.

It can also be seen from Fig. 3(a) that the Linked algorithm provides better IF estimation results than the Peak algorithm for SNR $\geq$ 1dB. The improved performance of the Linked IF estimator over the Peak algorithm can be attributed to the extra imposed constraint that component IF estimates for each time instant must be linked to a previous and a future local peak using the defined neighbourhood set in (20). As the SNR drops, the MBD may exhibit global peaks which are away from the true IF [6]. The component linking algorithm, instead, searches for significant local peaks that are linked, and this generally occurs in proximity to the true IF.

Divergence from the CRB for the Peak and WHT algorithms occurs for SNR $<$ 3dB and SNR $<$ 1dB respectively. The divergence points indicate the SNR at which the algorithms begin to breakdown. Therefore, it can be seen from Fig. 3(a) that both Linked and WHT algorithms break down at lower SNR than the Peak algorithm. For SNR = 1dB to 9dB, the WHT algorithm provides slightly better estimates than the Linked algorithm. This was expected as the variance associated with the resolution of the discrete QTFD can be reduced by estimating the underlying parametric IF function such as in the WHT-

based method[1]. However, for SNR > 9dB, the WHT exhibits a flat MSE. This error is determined by the resolution of the discrete Hough parameter space [25], which can be improved but at the expensive of an increase in computational load.

The results achieved by the algorithms when TFPF is applied, are shown in Fig. 3(b). It can be seen that the results are similar to the results when no preprocessing is applied, except for a shift towards lower SNRs. In this figure we have plotted the IF estimation error against the received signal SNR. The TFPF improves the SNR of the received signal by filtering out noise power. Therefore, a better IF estimate for the receive signal SNR is achievable because the TFPF preprocessing has improved the actual SNR. This is the reason for the shift towards lower SNR for the plots in Fig. 3(b).

3.2 Monocomponent Signal with Non-Parametric IF in WGN

In [9], it was stated that the Hough–Radon transform based IF estimator could be used to estimate any IF that satisfied a parametric constraint. This is true for any IF estimation technique which relies on the Hough transform of the TF representation such as those in [7–10].

A signal with an IF that is not easily parameterized is used for the sake of this performance assessment. The signal is of length $N = 1024$, and has a sampling rate of $f_s = 1$Hz. The signal was constructed with an IF which could be separated into three sections: hyperbolic frequency modulation (HFM), a constant tone and then LFM (see Fig. 4). The real discrete, amplitude and frequency modulated, signal used in this assessment is given by

$$s[n] = a[n]\cos(\phi[n]) \tag{23}$$

where the phase function is given by

$$\phi[n] = \begin{cases} \frac{2\pi 0.05}{-0.0017}\ln(1-0.0017n) \;:\quad 1 \le n \le 400 \\ \phi[400] + 2\pi 0.16(n-400) \;:\quad 401 \le n \le 624 \\ \phi[624] + 2\pi\left(0.16 + \frac{0.00035}{2}(n-624)\right)(n-624) \;:\quad 625 \le n \le 1024 \end{cases} \tag{24}$$

and the time–varying signal envelope by

$$a[n] = 1 + 0.075\cos(2\pi 0.00195n) \tag{25}$$

[1] This is analogous to the use of linear regression of observed data for improved estimation of a known, underlying, linear function.

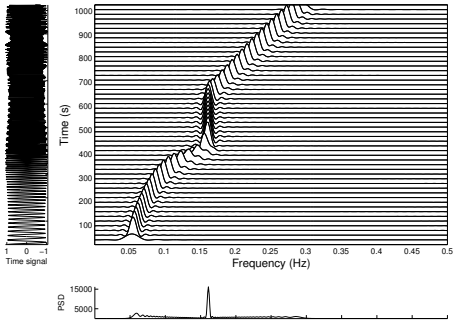

Fig. 4. Modified B-distribution of a synthetic monocomponent signal with amplitude modulation and non-parametric IF.

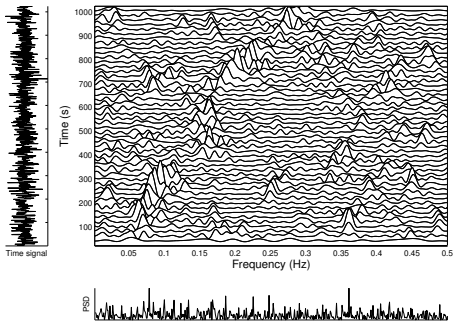

Fig. 5. Modified B-distribution of a noisy synthetic monocomponent signal with SNR = -9dB.

The MBD of the noise free, non–parametric IF signal is shown in Fig. 4.

Monte Carlo simulations (20 realizations with additive WGN) for varying levels of SNR revealed that the proposed IF estimation algorithm failed to link a component at SNR = 1dB with no preprocessing and SNR = -10dB when using TFPF preprocessing. The MBD of one realization of the noisy signal at -9dB is shown in Fig. 5. It can be seen that the distinct ridge following the IF law in Fig. 4 is now severely masked by the additive WGN in Fig. 5.

Fig. 6 shows the MBD of the noisy monocomponent signal after four iterations of the TFPF procedure. The window size for the pseudo–WVD was chosen to be 21 samples according to [16]. The IF estimate, extracted using the proposed algorithm, for the noise reduced signal in Fig. 6 is shown in Fig. 7.

A comparison with IF estimators based on the Hough transform was not undertaken for this signal as there is no way to easily parameterize the signal IF with sufficient accuracy. For example, if the true IF function is approximated with a 9^{th} order polynomial, which equates to a 10 dimensional Hough parameter space, the minimum MSE achievable, in the noise–free case and infinite Hough space resolution, is 6.92×10^{-6}. Compare this to Table 1 which shows the MSE for the Linked and Peak algorithms at SNR = 2dB with no preprocessing and SNR = -9dB using TFPF preprocessing. Table 1 also shows

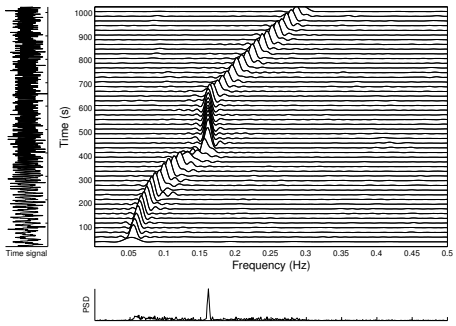

Fig. 6. Modified B-distribution of noisy monocomponent signal after four iterations of TFPF.

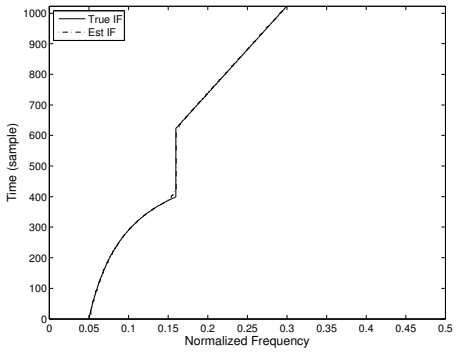

Fig. 7. True and Estimated IF of the monocomponent signal.

Table 1
Performance comparison of Peak and Linked algorithms with and without TFPF preprocessing.

	SNR	MSE	Bias	Variance
Peak	2dB	1.93×10^{-6}	-8.6×10^{-5}	1.91×10^{-6}
Linked	2dB	7.9×10^{-7}	-9.98×10^{-5}	7.8×10^{-7}
Peak (TFPF)	-9dB	1.07×10^{-6}	-9.3×10^{-5}	1.05×10^{-6}
Linked (TFPF)	-9dB	5.6×10^{-7}	-8.8×10^{-5}	5.5×10^{-7}

that the Linked algorithm provides a better estimate than the Peak algorithm. This improved performance is again attributed to the extra constraint that component IF estimates for each time instant must have linked local peaks.

3.3 Multicomponent Signal in WGN

The multicomponent signal used in this performance assessment consists of three components. The signal components include a LFM component, a sinusoidal frequency modulated component (SFM) and a hyperbolic frequency

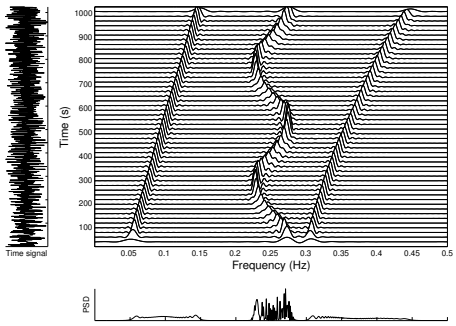

Fig. 8. Modified B-distribution of a synthetic multicomponent signal.

modulated component (HFM). The phase function for LFMs was presented in subsection 3.1. The phase function for a SFM is given by

$$\phi_{\mathrm{SFM}}(t) = 2\pi f_c t + \frac{m}{f_m}\sin(2\pi f_m t + \theta) \tag{26}$$

where f_c is the center frequency, m is the maximum variation, f_m is the sinusoidal modulation frequency and θ is the phase offset of the sinusoidal modulation. The phase function for a HFM is given by

$$\phi_{\mathrm{HFM}}(t) = \frac{2\pi f_0}{f_r}\ln|1 + f_r t| \tag{27}$$

where f_0 is the start frequency of the HFM and f_r is the hyperbolic frequency rate.

The synthetic signal is of length $N = 1024$ samples and has a sampling frequency of $f_s = 1$Hz. The time support for all components was the entire signal length. The phase functions and signal envelopes for each component are given by:

(1) LFM:

$$\phi[n] = 2\pi(0.05 + \frac{9.8\times10^{-5}}{2}n)n$$
$$a[n] = 1 + 0.075\cos(2\pi 0.00195n)$$

(2) SFM:

$$\phi[n] = 2\pi 0.25n + 12.5\sin(2\pi 0.002n)$$
$$a[n] = 1 + 0.075\cos(2\pi 0.00195n + 1)$$

(3) HFM:

$$\phi[n] = \frac{2\pi 0.3}{-3.3\times10^{-4}}\ln(1 - 3.3\times10^{-4}n)$$
$$a[n] = 1 + 0.075\cos(2\pi 0.00195n + 2.5)$$

Fig. 8 shows the MBD of the multicomponent signal used in this performance assessment. It can be seen from Fig. 8 that the MBD clearly shows the three signal components with minimal crossterms.

Monte Carlo simulations (20 realizations with additive WGN) for varying

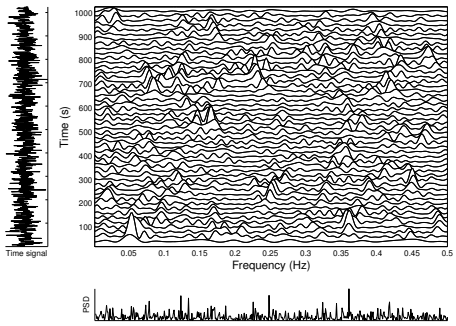

Fig. 9. Modified B-distribution of a noisy synthetic multicomponent signal with SNR = -11dB.

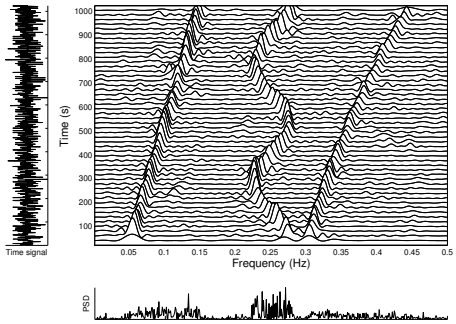

Fig. 10. Modified B-distribution of noisy multicomponent signal after four iterations of TFPF.

levels of SNR indicated that the Linked algorithm began failing to extract the IFs for the three components at SNR = 0dB with no preprocessing and SNR = -12dB with TFPF preprocessing. The MBD of one realization of the noisy signal, with SNR = -11dB, is shown in Fig. 9. It can be seen that the clear component ridges in Fig. 8 are now severely masked in Fig. 9.

The pseudo-WVD based iterative TFPF algorithm, repeated four times, was applied to the noisy signal for signal enhancement. A lag window length of 21 data points was chosen. The MBD of the estimated signal from the iterative TFPF procedure is shown in Fig. 10. It can be seen from Fig. 10 that the signal components are now distinguishable from the reduced noise level.

Fig. 11 shows the binary image, $B(t, f)$, obtained from the detection of local peaks of the MBD in Fig. 10. It can be seen from Fig. 11 that many local peaks exist in the TF representation. However, only the signal components are linked from approximately the beginning of the signal to the end. Fig. 12 shows the estimated IFs of the linked components and the true IF of the signal components.

A comparison with IF estimators based on the Hough transform of the TF representation could not be made for this example as each of the signal components exhibit different parametric functions. That is, if the TF representation

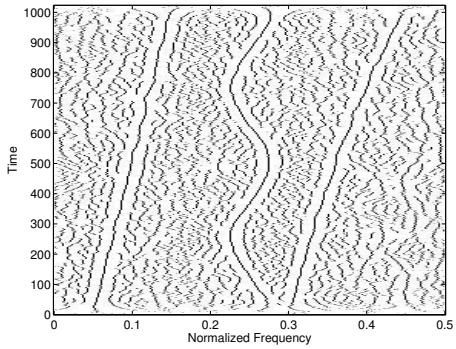

Fig. 11. Binary image indicating the locations of the local peaks in Fig. 9.

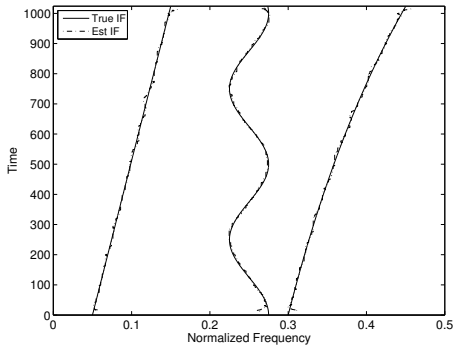

Fig. 12. True and Estimated IFs of the multicomponent signal.

Table 2
Performance of Linked algorithm for noisy multicomponent signals, with and without TFPF preprocessing.

	SNR	MSE	Bias	Variance
LFM	1dB	2.56×10^{-6}	1.53×10^{-5}	2.54×10^{-6}
SFM	1dB	2.93×10^{-6}	4.15×10^{-5}	2.91×10^{-6}
HFM	1dB	5.78×10^{-6}	-3.9×10^{-5}	5.6×10^{-6}
LFM (TFPF)	-11dB	1.7×10^{-6}	-4.3×10^{-5}	1.7×10^{-6}
SFM (TFPF)	-11dB	2.0×10^{-6}	4.4×10^{-5}	1.99×10^{-6}
HFM (TFPF)	-11dB	2.6×10^{-6}	-1.1×10^{-4}	2.58×10^{-6}

was transformed to the Hough line space, even in the noise–free case, only an accurate estimate for the LFM could be obtained. A comparison with the Peak algorithm could not be made as the signal exhibits multiple components. However, using the TFPF preprocessing, the proposed IF estimation scheme can provide accurate estimates down to SNR = -11dB. For SNR > -11dB, the algorithm begins failing to link the IFs of signal components. The IF estimation results with and without TFPF are shown in Table 2.

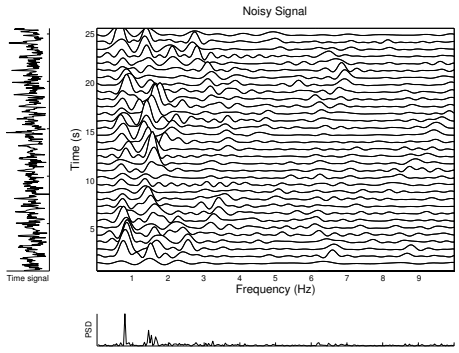

Fig. 13. Time–frequency representation of noisy newborn EEG seizure epoch.

3.4 Application of IF Estimator to Newborn EEG Seizure

The multicomponent characteristic of newborn EEG was reported in [26] and studied in detail in [13]. The number of components and the IF of signal components are important features characterizing the newborn EEG seizure. Extraction of this information using QTFDs has, previously, been a difficult and time consuming task involving supervised local peak estimation using subjective thresholding and subjective determination of the number of signal components. However, using the proposed IF estimation scheme, this information can be extracted automatically in an objective manner.

The newborn EEG data used in this section was recorded at the Royal Brisbane and Women's Hospital in Brisbane, Australia. The raw EEG data was sampled at 256Hz. However, the majority of spectral energy in the newborn EEG (*i.e.* $\geq 95\%$ of spectral energy) is concentrated in the first two frequency bands (δ and θ), which consist of frequencies between 0.4-8Hz [27]. Therefore, the raw EEG was low pass filtered, with a cutoff frequency at 8Hz, before being down sampled to 20Hz.

Fig. 13 shows the MBD of an epoch of noisy newborn EEG seizure. This TF representation does not reveal any clear signal components which have been previously documented in [13, 26]. Fig. 14 shows the MBD of the enhanced signal after the TFPF procedure. Subjective analysis, through visual inspection of the TF representation, suggests that there are two signal components. Fig. 15 shows the results of the proposed IF estimation method. It can be seen from Fig. 15 that two components have been extracted from the signal and their individual IFs have been estimated. This information was extracted automatically and did not require any supervision.

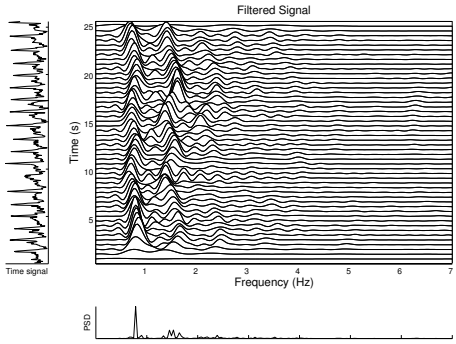

Fig. 14. Time–frequency representation of noisy newborn EEG seizure epoch after TFPF.

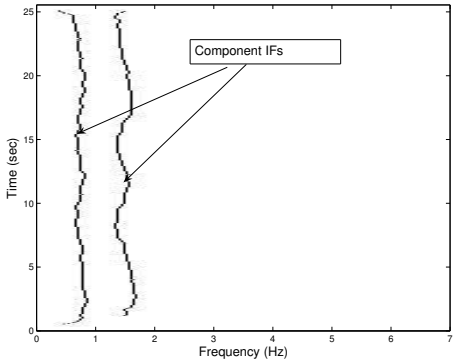

Fig. 15. IF estimates of the two component newborn EEG seizure signal.

4 Classification and Parameter Estimation of Signal Components

Classification is a very important application in signal and image processing. For nonstationary signals, IFs of signal components are often very informative and can be used as features in signal classification [13,26]. To show a potential application of the proposed IF estimation technique for multicomponent signals, we propose a signal classification method based on the IF estimates of a multicomponent signal. The classification process is composed of the following stages: IF estimation, IF modelling, and classification of the IF based on the estimated model parameters. The proposed classification method is applied to both synthetic and real signals. It should be noted here that many other applications of the proposed IF estimation technique are possible. Examples of applications include: detection, filtering and signal synthesis. Since the first stage of the classification process has been detailed in section 2, we now discuss the two remaining stages.

4.1 IF modelling

A signal component class, defined by its IF, is any set of functions [8]

$$C = \left\{ a(t) e^{j2\pi \int_{-\infty}^{t} f_{i,C}(\tau;\psi) d\tau} \right\}_{\psi \in \Psi} \tag{28}$$

where $f_{i,C}$ is an IF functional model defining the class. The IF functional model is parameterized by an L-dimensional vector, ψ, where Ψ is the set of all valid vectors for the IF class model $f_{i,C}$. The dimension, L, of the parameter vector is class dependent. Three examples of component classes, (LFM, SFM and HFM), were defined earlier in section 3. The IF functional models, $f_{i,C}(t)$ and the parameter vectors, ψ, for the LFM, SFM and HFM classes are expressed as:

(1) LFM: $f_{i,\mathrm{LFM}}(t) = f_0 + f_r t$, $\psi = [f_0, f_r]$.
(2) SFM: $f_{i,\mathrm{SFM}}(t) = f_c + m\cos(2\pi f_m t + \theta)$, $\psi = [f_c, m, f_m, \theta]$.
(3) HFM: $f_{i,\mathrm{HFM}}(t) = \frac{f_0}{1+f_r t}$, $\psi = [f_0, f_r]$.

Many other classes of IF law for signal components may be defined including *quadratic, cubic, higher order polynomial* and *piecewise linear.*

4.2 Parameter Estimation and Classification

The first step in automatic signal classification requires the formation of signal classes based on the observed characteristics. For example, if a real signal can exhibit J classes of IF law, the set of IF functional classes can be defined as

$$D = \{C_v\}_{v=1,2,\ldots,J} \tag{29}$$

The next step is to find the optimal parameter vector, $\bar{\psi}$, (and therefore optimal IF function, $\bar{f}_{i,C_v}(t)$) for each $C_v \in D$, that fits the estimated IF, $\hat{f}_i(t)$, in a least squares sense.

The fitting of data to linear lines, and more generally polynomial functions, using least squares fitting is a well established technique [28]. However, the fitting of data to nonlinear models (nonlinear parameter estimation) is more complicated. To find $\bar{\psi}$, (and $\bar{f}_{i,C_v}(t)$) for each $C_v \in D$, we have used a Large–Scale optimization algorithm that is a subspace trust region method based on the interior–reflective Newton method [29]. This method was chosen as it allows for setting upper and lower bounds on the L parameter vector variables, unlike Medium–Scale algorithms such as the Gauss–Newton and Levenberg–Marquardt methods [30].

Table 3
Parameter estimation results for noisy multicomponent signals

Component	ψ	True Value	Estimate Values	
			mean	std
LFM	f_o	0.05	0.0499	2.58e–4
	f_r	9.766e–5	9.775e–5	4.731e–7
SFM	f_c	0.25	0.2499	8.725e–5
	m	0.025	0.0243	1.762e–4
	f_s	0.002	0.002	2.780e–4
	θ	0.0	–0.0129	0.0094
HFM	f_o	0.3	0.3002	1.038e–4
	f_r	–3.258e–4	–3.250e–4	5.697e–7

Signal components are classified using the MSE between the optimal IF parametric model in each class, $\bar{f}_{i,C_v}[n]$, and the estimated IF of the component, $\hat{f}_i[n]$. The signal component class is determined as

$$\arg \min_{C_v \in D} \left\{ \sum_n \left(\bar{f}_{i,C_v}[n] - \hat{f}_i[n] \right)^2 \right\} \tag{30}$$

4.2.1 Synthetic Signals

To demonstrate the proposed classification procedure, testing was conducted on twenty synthetic, noisy, multicomponent signals. The deterministic part of the multicomponent signals used in this section consist of the same LFM, SFM and HFM components used in section 3 (see Fig. 8). Twenty realizations of real stationary white Gaussian noise with a SNR of -9dB, were each individually added to the deterministic part to form the twenty signals.

In this demonstration, it was assumed *a priori* analysis revealed $J = 3$ classes of IF law were exhibited by the synthetic signal; LFM, SFM and HFM components. In this example, accuracy of IF component classification and accuracy of parameter estimation were tested.

The classification procedure provided an excellent IF component classification rate of 100% in this demonstration. That is, every component was correctly classified into either LFM, SFM or HFM. The parameter estimation results are summarized in Table 3, showing the true value for each parameter, and the mean and standard deviation (std) of the estimated values over the twenty noisy signals. It can be seen from Table 3 that accurate estimates of the parameter values for the deterministic components were acheived for each of the noisy multicomponent signals.

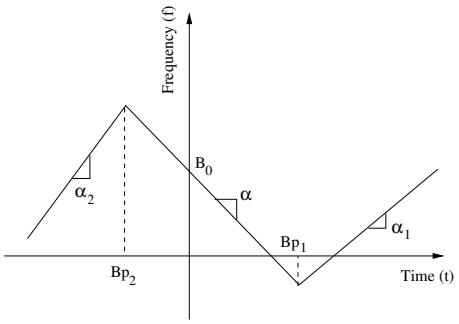

Fig. 16. Illustration of three piece PLFM function parameters.

4.2.2 Newborn EEG Signal

Classification of the newborn EEG seizure components was first attempted in [31] and further detailed in [26]. In [26,31], the newborn EEG were subjectively classified into various forms of LFM patterns which included:

- LFM patterns with quasi–constant frequency.
- Short LFM patterns with quasi–constant frequency.
- LFM patterns with a decreasing pattern.
- Piecewise LFM patterns.

It was shown clearly in [13], however, that newborn EEG seizure has a number of LFM patterns with increasing frequency, which was left out of the classification set in [26, 31].

The proposed component classification procedure was applied to the newborn EEG seizure signal. According to the subjective classification of newborn EEG seizure components in [13, 26, 31, 32], the only classes of IF law exhibited in newborn EEG seizure are LFM and piecewise LFM (PLFM)[2] (*i.e.* $J = 2$). The IF model, $f_i(t)$ for the three piece PLFM class of functions is expressed as [32]

$$f_i(t) = \frac{\alpha_1 - \alpha}{2}|t - Bp_1| + \frac{\alpha - \alpha_2}{2}|t - Bp_2| + \frac{\alpha_1 + \alpha_2}{2}t - \frac{\alpha_1}{2}Bp_1 - \frac{\alpha_2}{2}Bp_2 + B_0 \tag{31}$$

where $\psi = [\alpha, \alpha_1, \alpha_2, Bp_1, Bp_2, B_0]$. The parameters of the function are demonstrated in Fig. 16. However, in our classification of the newborn EEG signal components, both the SFM and HFM classes of functions were included (*i.e.* $J = 4$).

The newborn EEG seizure component with the lowest frequency content (see Fig. 15), referred to from here on as component one, was classified as a PLFM

[2] A sufficient number of LFM pieces for approximately a 20 second period of EEG seizure was found to be three [32]. Therefore, the three piece PLFM class of functions was used for classification.

component. This objective result supports the previous subjective findings of [13, 26, 31, 32]. However, the second component was classified as an SFM component according to the proposed classification scheme. This is a new finding. It also shows the potential of this technique for further classification of newborn EEG seizure components, which will be utilized in future research.

5 Discussion and Conclusion

The marriage of image processing techniques and TF representations appears highly suitable for IF estimation. Previous attempts of applying image processing techniques to TF representations, [7–10], have all employed some modified version of the Hough transform to estimate the IF and parameterize the IF function. However, many limitations arise when using the Hough transform of the TF representation for IF estimation. That is, *a priori* knowledge of component IF class is required for accurate IF estimation, only one class of the IF law can be exhibited by the signal for IF estimation, and only poor IF estimation can be achieved for signal components with IF laws that aren't easily represented by a parametric function. Hough transform–based techniques also require threshold setting for extraction of signal components from the Hough space. Therefore, components may be missed if the IF of the component does not exactly follow a function represented in the Hough parameter space, or the noise level becomes too high.

Earlier local TF peak detection–based techniques for IF estimation of multicomponent signal, such as [12], require a threshold to be set so that local maxima caused by crossterms and noise can be ignored. It was noted in [12] that the threshold level is application (signal) and distribution dependent and requires a prior TF analysis of the signal to locate true components, done manually, to define an appropriate threshold level. The component linking procedure removes the need for setting threshold levels in the TF domain. Therefore, the proposed IF estimation algorithm is useful in automatically and objectively determining the number of signal components and estimating their individual IFs. By employing TFPF for signal enhancement, it was also shown that the proposed IF estimation algorithm can still obtain accurate estimates of component IFs in low SNR environments. We note that the TFPF procedure requires oversampling of the signal for accurate filtering. This may be a disadvantage in some real applications, particularly when the oversampled signal is not available.

A desirable aspect of the Hough transform–based IF estimation techniques for some is the ability to parameterize the IF function. Once again, however, accurate parameterization can only occur for multicomponents that are from the same class of functions. In this paper, we proposed a method, based on

linear and nonlinear least squares data–fitting, which allows for: 1) the classification of multicomponent which belong to differing classes and 2) accurate parameter estimation of the individual components.

The proposed method of IF extraction presented in this paper is generic and may be applied to any TF representation. In this paper, the MBD was chosen as it provides a high resolution, reduced interference TF representation.

In summary, a TF based technique for multicomponent IF estimation which incorporates simple, yet effective, image processing techniques was developed in this paper. The technique overcomes many of the limitations associated with other TF based multicomponent IF estimators. A method for signal component classification and parameter estimation, incorporating the proposed IF estimation technique, was also presented. The proposed classification procedure may be used in many real applications such as newborn EEG seizure classification.

6 Aknowledgments

The authors would like to acknowledge Prof. Paul Colditz (Perinatal Research Centre), Dr. Chris Burke and Jane Richmond (Royal Children's Hospital, Brisbane, Australia) for organizing the aquisition of real newborn EEG seizure data used in this paper.

References

[1] B. Boashash, Estimating and Interpreting the Instantaneous Frequency of a Signal-Part 1: Fundamentals, Proceedings of the IEEE 80 (4) (1992) 520–538.

[2] J. J.L Brown, Analytic Signals and Product Theorems for Hilbert Transforms, IEEE Transactions on Circuits and Systems 21 (6) (1974) 790–792.

[3] B. Boashash, Estimating and Interpreting the Instantaneous Frequency of a Signal-Part 2: Algorithms and Applications, Proceedings of the IEEE 80 (4) (1992) 540–568.

[4] B. Ristic, B. Boashash, Instantaneous Frequency Estimation of Quadratic and Cubic FM Signals using the Cross Polynomial Wigner-Ville Distribution, IEEE Transactions on Signal Processing 44 (6) (1996) 1549–1553.

[5] V. Katkovnik, L. Stanković, Instantaneous Frequency Estimation Using the Wigner Distribution with Varying and Data Driven Window Length, IEEE Transactions on Signal Processing 46 (9) (1998) 2315–2325.

[6] V. Ivanović, M. Daković, L. Stanković, Performance of quadratic time–frequency distributions as instantaneous frequency estimators, IEEE Transactions on Signal Processing 51 (1) (2003) 77–89.

[7] S. Barbarossa, Analysis of Multicomponent LFM Signals by a Combined Wigner–Hough Transform, IEEE Transactions on Signal Processing 43 (6) (1995) 1511–1515.

[8] S. Barbarossa, O. Lemoine, Analysis of Nonlinear FM Signals by Pattern Recognition of Their Time–Frequency Representation, IEEE Signal Processing Letters 3 (4) (1996) 112–115.

[9] R. M. Rangayyan, S. Krishnan, Feature identification in the time–frequency plane by using the Hough–Radon transform, Pattern Recognition 34 (6) (2001) 1147–1158.

[10] N. Bennett, N. Saito, Using edge information in time–frequency representations for chirp parameter estimation, Applied and Computational Harmonic Analysis 18 (6) (2005) 1147–1158.

[11] B. Boashash, Heuristic formulation of TFDs, in: B. Boashash (Ed.), Time–Frequency Signal Analysis and Processing: A Comprehensive Reference, Elsevier, London, 2003, Ch. 2, pp. 29–57.

[12] Z. Hussain, B. Boashash, Adaptive instantaneous frequency estimation of multicomponent FM signals using quadratic time–frequency distributions, IEEE Transactions on Signal Processing 50 (8) (2002) 1866–1876.

[13] L. Rankine, N. Stevenson, M. Mesbah, B. Boashash, A Nonstationary Model of Newborn EEG, IEEE Transactions on Biomedical Engineering, accepted.

[14] M. Malarvili, M. Mesbah, B. Boashash, Time-frequency distribution moments of heart rate variability for neonatal seizure detection, in: Proc. IEEE ICASSP, Vol. 3, 2006, pp. 149–152.

[15] J. Illingworth, J. Kittler, A Survey of the Hough Transform, Computer Vision and Graphical Image Processing 44 (1) (1988) 87–116.

[16] B. Boashash, M. Mesbah, Signal Enhancement by Time–Frequency Peak Filtering, IEEE Transactions on Signal Processing 52 (4) (2004) 929–937.

[17] B. Boashash, Theory of quadratic TFDs, in: B. Boashash (Ed.), Time–Frequency Signal Analysis and Processing: A Comprehensive Reference, Elsevier, London, 2003, Ch. 3, pp. 59–81.

[18] B. Boashash, Time–frequency concepts, in: B. Boashash (Ed.), Time–Frequency Signal Analysis and Processing: A Comprehensive Reference, Elsevier, London, 2003, Ch. 1, pp. 4–27.

[19] M. Arnold, M. Roessgen, B. Boashash, Signal Filtering using Frequency Encoding and the Time–Frequency Plane, in: Proc. Asilomar Conf., Pacific Cove, CA, 1993, pp. 1459–1463.

[20] A. Farag, E. Delp, Edge linking by sequential search, Pattern Recognition 28 (5) (1995) 611–633.

[21] T. Acharya, A. Ray, Image Processing: Principles and Applications, Wiley Interscience, Hoboken, NJ, 2005.

[22] B. Boashash, G. Putland, Discrete time–frequency distributions, in: B. Boashash (Ed.), Time–Frequency Signal Analysis and Processing: A Comprehensive Reference, Elsevier, London, 2003, Ch. 6.1, pp. 232–241.

[23] M. Roden, Analog and Digital Communication Systems, 4th Edition, Prentice Hall, Upper Saddle River, NJ, 1996.

[24] S. Peleg, B. Porat, B. Friedlander, The Achievable Accuracy in Estimating the Instantaneous Phase and Frequency of a Constant Amplitude Signal, IEEE Transactions on Signal Processing 41 (6) (1993) 2216–2224.

[25] R. Agrawal, R. Shevgaonkar, S. Sahasrabudhe, A fresh look at the Hough transform, Pattern Recognition Letters 17 (10) (1996) 1065–1068.

[26] B. Boashash, M. Mesbah, A time-frequency approach for newborn seizure detection, IEEE Engineering in Medicine and Biology Magazine 20 (5) (2001) 54–64.

[27] M. Scher, M. Sun, D. Steppe, R. Guthrie, R. Sclabassi, Comparison of EEG spectral and correlation measures between healthy term and preterm infants, Pediatric Neurology 10 (2) (1994) 104–108.

[28] P. Lancaster, K. Šalkauskas, Curve and Surface Fitting: An Introduction, Academic Press, London, 1986.

[29] T. Coleman, Y. Li, An Interior Trust Region Approach for Nonlinear Minimization Subject to Bounds, SIAM Journal on Optimization 6 (2) (1996) 418–445.

[30] P. Gill, W. Murray, M. Wright, Practical Optimization, Academic, New York, 1981.

[31] B. Boashash, M. Mesbah, P. Colditz, Newborn EEG seizure pattern characterisation using time-frequency analysis, in: Proc. IEEE International Conference on Acoustics, Speech ad Signal Processing, Salt Lake City, USA, 2001, pp. 1041–1044.

[32] P. Celka, P. Colditz, Nonlinear nonstationary Wiener model of infant EEG seizures, IEEE Transactions on Biomedical Engineering 49 (6) (2002) 556–564.